New insights on the Messina 1908 seismic source from postseismic sea level change

V. Cannelli, D. Melini, A. Piersanti

Istituto Nazionale di Geofisica e Vulcanologia, Via di Vigna Murata 605, I-00143 Rome, Italy

3 April 2013

SUMMARY

The identification of a source model for the catastrophic 28 December 1908 Messina earthquake ($M_w = 7.2$) has been the subject of many papers in the last decades. Several authors proposed different models on the basis of seismological, macroseismic and geodetic datasets; among these models, remarkable differences exist with regard to almost all parameters. We selected a subset of six models among those most cited in literature and used them to model the postseismic sea level variation recorded at the tide gauge station of Messina (until 1923), in order to attempt an independent discrimination among them. For each model we assumed a simple rheological structure and carried out a direct-search inversion of upper crust thickness and lower crust viscosity to fit the postseismic sea level signal. This approach enabled us to identify a class of fault geometries which is consistent with the postseismic signal at the Messina tide-gauge and with the known structural and rheological features of the Messina strait.

Key words: Sea level change – Rheology: crust and lithosphere – Earthquake source observations.

1 INTRODUCTION

On December 28th, 1908, the Messina region was struck by one of the strongest and most catastrophic earthquakes in the seismic history of Italy, with an estimated moment magnitude between

7.0 and 7.2 (Boschi et al. 1997; Pino et al. 2000) and a MCS maximum intensity of XI (Boschi et al. 1997). The earthquake and the subsequent tsunami, that reached a maximum run-up height exceeding 10 meters (Baratta 1910), caused over 60,000 casualties (Mercalli 1909). Although the earthquake was a local Italian event, it drew the attention of the international scientific community since the first decades of the 20th century. The amount of available literature, mostly contemporaneous with the event, proves its exceptional impact not only in the geoscience community, but also in the economic and social fields. The bibliography, restricted to geoscience studies, consists of about 300 publications, including scientific articles and monographic studies. All the currently available scientific and technical information on the 1908 Messina earthquake (also known as the 1908 Messina and Reggio Calabria earthquake) is, therefore, the result of a century of studies. Recently, two works had as objective the critical organization of the huge amount of acquired knowledge about the Messina earthquake. The first is the book of Bertolaso et al. (2008), which was published to celebrate the earthquake centennial and collects contributions worked out from different points of view (seismological analyses, effects, perspectives and bibliographic records). The second is the scientific article of Pino et al. (2009), which describes in detail the historical path followed by investigations on this earthquake, in parallel to the evolution of seismology as a research discipline; this work raised some criticisms (Amoruso et al. 2010; Pino et al. 2010), testifying that several aspects of the Messina earthquake are still subject to debate. We refer the readers to the aforementioned literature (and to references therein) for a more detailed review and for a broader description of the 1908 Messina earthquake.

The idea of the present work arises from the observation that the Messina tide-gauge station operating in the time period 1896-1923 recorded a strong continuous postseismic signal lasting about 15 years after the earthquake and this represents a quite uncommon feature in historic tide-gauge records. Platania (1909) was the first author who reported the tide gauge records of the tsunami in the Mediterranean Sea from different stations (Palermo, Naples, Civitavecchia, Ischia, and Malta) in order to estimate the period and directivity of the tsunami waves. Omori (1913) also presented some results about the mean height of sea level at some Italian tide gauge stations (including Messina) and the influence of 1908 Messina earthquake on it. Tide gauge data in the

Messina harbor were also employed by Mulargia & Boschi (1983), and afterwards by Bottari et al. (1992) and De Natale & Pingue (1991), to give an interpretation of a land uplift since 1897 till 1900, a subsidence since 1900 till 1908 and a new uplift since 1912 till 1918, at an higher rate.

In the past decades, several source models for the Messina earthquake have been published in literature, on the basis of different observation datasets (Schick 1977; Mulargia & Boschi 1983; Bottari et al. 1986; Capuano et al. 1988; Valensise 1988; Boschi et al. 1989; De Natale & Pingue 1991; Valensise & Pantosti 1992; Pino et al. 2000; Amoruso et al. 2002). These models propose fault planes geometries with remarkable differences with regard to almost all parameters and it is evident that a widespread agreement on the actual fault geometry has not been reached yet (e.g., Amoruso et al. 2010; Pino et al. 2010). The aim of this work is to attempt a discrimination among a subset of these fault models, by using each of them to fit the postseismic tide gauge data through the inversion of a simple rheological profile. While the exact characterization of the 1908 Messina earthquake still remains an open issue, our analysis is focused on a signal that has not yet been considered in the seismological studies on Messina seismic source, and can thus provide an independent indication of which class of fault geometries is more consistent with the geodynamic context of the region.

2 THE MESSINA TIDE-GAUGE DATA

The Mati-Ricci tide gauge station of Messina, recording sea level from 1897, was destroyed by the 1908 earthquake and by the subsequent destructive tsunami (Omori 1913). After the earthquake, the tide gauge station was restored, providing postseismic data from April 1909 until February 1923 (IDROMARE, http://www.idromare.it/). Nearest available tidal data in the same period came from Palermo (1896-1922) and Catania (1896-1920), both Mati-Ricci type stations (IDROMARE, http://www.idromare.it/), located at epicentral distances of 195 and 87 km, respectively. Tide gauge time-series have been made available by the Permanent Service for Mean Sea Level (PSMSL, http://www.psmsl.org/) (Woodworth & Player 2003), the global data bank for long term sea level change information from tide gauges and bottom pressure recorders. PSMSL distributes both the Revised Local Reference (or RLR) data and metric data. The RLR data set has been reduced to

a common datum and checked for inconsistencies or erroneous data by the PSMSL, whereas the metric data set is the raw data entered in the PSMSL databases for each station, directly as received from local authorities. Since Messina is a 'metric only' station, the choice of metric dataset was unavoidable; but on the other hand the RLR dataset, usually superior to the metric, is not essential here, because no analysis or interpretation of absolute sea level data is made in this work.

In Fig. 1 we show the monthly mean sea level (hereafter MMSL) at tide gauge stations of Messina, Palermo and Catania for the period 1896-1923. A vertical black line marks the occurrence time of the 1908 event. The postseismic data window (1909-1923) is sufficient to evidence a visible change in the Messina MMSL signal (black circles) in comparison with the pre-seismic trend. Data from Palermo and Catania tide gauge stations do not show the same variation. These observations are compatible with the interpretation of the 1908 earthquake as a local event; in fact several studies suggest that the 1908 earthquake was accompanied by significative coseismic subsidence only at Messina coasts (Loperfido 1909; Mulargia & Boschi 1983; Bottari et al. 1989, 1992). Recently, Olivieri et al. (2013) analyzed a newly disclosed sea level record from the Mazara del Vallo tide gauge, and found a trend change point in late 1909, which however the authors interpreted as an oceanic signal.

3   SEISMIC SOURCE MODELS

The seismic source of the 1908 Messina earthquake has been thoroughly investigated in literature during the last decades (see Bertolaso et al. (2008) and Pino2009 for a review). In this study, we selected six source models, obtained respectively on the basis of seismological data (Schick 1977), macroseismic methods (Bottari et al. 1986), leveling observations (Capuano et al. 1988; Boschi et al. 1989; De Natale & Pingue 1991) and joint inversion of seismological and geodetic data (Amoruso et al. 2002). The rationale behind this choice is the availability of the whole set of source parameters that are required for a quantitative modeling of postseismic deformation, as we will discuss below. Piatanesi et al. (1999) and Tinti et al. (1999) already investigated the tsunamigenic potential of models by Boschi et al. (1989) and Capuano et al. (1988) and found that both seismic sources are unable to explain the overall observed height of the tsunami, underestimating the

maximum wave heights by a factor of 4-5 with respect to the actual run-ups. In their more recent contribution to Bertolaso et al. (2008), the authors carried out a forward numerical simulation of the tsunami wave propagation considering two seismic sources (Boschi et al. 1989; Amoruso et al. 2002), an underwater landslide source model (Billi et al. 2008) and combinations of seismic source and underwater landslide models. All the considered simulations failed to explain all aspect of observed data, leaving the determination of the tsunamigenic source a still unsolved problem.

All the considered models, with their source parameters, are summarized in Table 1; the position and extents of sources are shown in Fig. 3. In what follows, we will indicate each source model with the first letter of the author name followed by the last two digits of the publication year, for instance S77 will stand for Schick (1977). These abbreviations are reported in Table 1 for convenience.

From Table 1 we see that remarkable differences exist among the proposed models, with regard to almost all the source parameters. Both models S77 and B86 suggest a westward-dipping fault, the first roughly parallel to the eastern Sicilian coast and with an approximately E-W extension, the second slightly eastward rotated and with a SE-NW extension. Models C88, B89 and DN91, which are all derived from leveling observations, indicate an east-dipping fault, with B89 suggesting a fault strike roughly parallel to the eastern Sicilian coast, while C88 and DN91 have a slightly westward rotated fault plane. Model A02, resulting from a "modern" joint inversion of seismological and geodetic data, has an orientation similar to C88 and DN91.

The size of fault planes listed in Table 1 varies widely over the proposed models. The largest plane, with an area of 2100 km^2 is the one of model DN91, which has been obtained essentially enlarging the same structure of C88. The smallest fault plane, with an area of 450 km^2, corresponds to model S77, which was the first model obtained with modern seismological techniques using existing instrumental data. Fault lengths range from about 30 to 70 km, while fault widths are more constrained between 20 and 30 km. The fault depth is another debated issue: in model S77, the shallow edge of rupture plane reaches the surface; for models C88, DN91 and A02 a blind (but shallow) rupture is assumed, while in models B89 and B86 a deeper fault plane is obtained, with top edge at depths of 4 km and 16 km, respectively. Finally, we point out that for each of the six

models, the city of Messina is always just above (or very close to) one of the edges of the fault planes.

4   METHODS

4.1   Sea level change modeling

By definition, the *sea level change* at a point of coordinates ω at time t is given by (Spada & Stocchi 2006, and references therein):

$$S(\omega, t) = SL(\omega, t) - SL_0 \tag{1}$$

where $SL(\omega, t)$ is the offset between the sea surface and that of solid Earth at position ω and time t, i.e. the sea level variation that would be measured by a stick-meter, and SL_0 is a reference sea level, measured at the same point but at a remote reference time t_0. Eq. 1 can also be written as:

$$S(\omega, t) = N(\omega, t) - U(\omega, t) \tag{2}$$

where N is the sea surface displacement, i.e. the sea level variation that would be measured by a satellite altimeter, and U is the vertical displacement of the solid surface of the Earth. If we consider alterations of the shape of the geoid small and negligible compared to vertical displacements of the surface topography (Melini & Piersanti 2006; Melini et al. 2010), a positive variation of sea level, as in the case of Messina MMSL, implies a negative variation of the vertical displacement (i.e. a subsidence).

From Fig. 1 it is evident that an annual modulation, presumably of tidal origin, is present in all the considered sea level time-series. In order to improve the reliability of our inversion, we decided to remove this periodic signal by modeling the differences between the sea level time-series at Messina and those at a nearby PSMSL site; this is a viable approach only if the periodic tidal signal is uniform across the considered region. In order to verify this assumption, we extracted PSMSL monthly tidal records in the time window 2001-2011 for Palermo-II, Porto Empedocle, Catania-II and Messina-II tide gauge stations and plotted them in Fig. 2. The first three sites are located approximately at the middle of northern, southern and eastern sicilian coasts, respectively,

while the last site is located at the strait, so these four tide gauges are well representative of the different tidal subsystems of Sicily (Pinardi et al. 1997; Carillo et al. 2012). From Fig. 2 it is clear that a coherent periodic signal is present at all considered sites, demonstrating that the same uniform long-period tidal modulation is acting on the considered region; it is therefore safe to filter out this signal by considering the difference between pairs of tide gauge records. With the PSMSL data of Fig. 1 we can therefore build the following quantity:

$$\Delta S(t) = \left(S_{ME}(t) - S_{ME}^0\right) - \left(S_{TF}(t) - S_{TF}^0\right) \tag{3}$$

where $S_{ME}(t)$ and $S_{TF}(t)$ are the postseismic MMSLs at the Messina tide gauge station (ME) and at the tide gauge station used for tidal filtering (TF), while S_{ME}^0 and S_{TF}^0 represent the estimated sea level just before the earthquake occurrence, which are subtracted from the corresponding time-series in order to refer them to a common baseline. Since from 1909 to 1923 the Catania MMSL record shows more missing data with respect to Palermo MMSL record (see also Fig. 1), we choose Palermo as tidal filter station. The resulting postseismic sea level variation ΔS for Messina (black circles) is compared to the unfiltered postseismic MMSL (red circles) in Fig. 4; most of the periodic component superimposed on the postseismic signal has been canceled out with this simple filtering scheme.

4.2   Inversion procedure

In this section we describe the method we used to obtain, for each source model listed in Table 1, a best-fitting prediction of the sea level signal.

We defined a 3-layer (variable) rheological structure, described in Table 2, characterized by an elastic upper crust, a viscoelastic lower crust and a viscoelastic half-space representing the upper mantle. The interface between the first two layers is allowed to vary between 2 and 20 km, while the second interface is fixed at 220 km. The Maxwell viscosity of the lower crust is also allowed to vary between 10^{16} and 10^{19} Pa s, whilst the upper mantle viscosity is kept fixed at 10^{20} Pa s. For a given choice of upper-lower crust boundary depth (z) and lower crust viscosity (η), we computed the predicted sea level time-series using the postseismic rebound model proposed by Wang et al. (2006), which employs the Thomson-Haskell propagator method to solve the

boundary-value problem associated with gravitationally self-consistent deformations induced by a seismic dislocation. In this way, for any of the source models of Table 1, we can define a misfit

$$\chi_m^2(z, \eta) = \sum_{i=1}^{n} (\Delta S(t_i) - \Delta S_m(t_i, z, \eta))^2 \qquad (4)$$

where m is a given model, n is the number of data points, $\Delta S(t_i)$ is the postseismic sea level variation defined in eq. 3 and $\Delta S_m(t_i, z, \eta)$ is the predicted sea level signal at time t_i using source model m and rheology profile defined by z and η. According to equations 2 and 3,

$$\Delta S_m = (N_m^{ME} - U_m^{ME}) - (N_m^{PA} - U_m^{PA}) \qquad (5)$$

where N_m^x and U_m^x are the sea surface perturbation and the vertical deformation obtained with source model m at tide-gauge station x, respectively, with x being Messina (ME) or Palermo (PA). The dependence upon t, z and η has been left implicit.

For each source model, we obtained the values of z and η which minimize the misfit $\chi_m^2(z, \eta)$ through a direct-search of the parameter space (z, η). The crustal thickness z has been varied between 2 and 20 km, while the lower crust viscosity has been sampled logarithmically, with $\log(\eta/1\ Pa\ s)$ varying between 16 and 19. The sampling of the parameter space has been performed with the Neighborhood Algorithm (hereafter NA) (Sambridge 1999a,b), which provides a computationally efficient direct-search scheme by automatically increasing the sampling density in regions of local minima, ensuring at the same time robustness against incomplete convergence to a local minimum.

5   RESULTS

Since the evaluation of forward models is a time-consuming process, the direct-search of the parameter space (z, η) represents a very intensive computational task. For this reason, even using a parallel version of the NA sampler on a distributed-memory cluster, we must find a trade-off between sampling density and computational time. We set up the NA algorithm with an initial sample of $N_0 = 200$ random points in the (z, η) space, and performed $N_i = 20$ iterations resampling the 100 lowest-misfit Voronoi cells with $N_r = 100$ new models (see Sambridge 1999a,b, for details). In this way, at the end of the sampling process, the number of generated models is

$N_0 + N_i N_r = 2200$; the sampling process requires about 36 hours using 256 CPU cores. With these settings, the sampling follows an explorative strategy, avoiding the risk of finding a local minimum. We verified that the global minimum is found well before the end of the sampling algorithm, ensuring that the sample size is adequate.

As we discussed before, for all the considered source models, the city of Messina is always close to a fault plane edge (see Fig. 3). In these conditions, the modeled signal at the Messina tide-gauge may be affected by spurious boundary effects, which we expect to be stronger for the coseismic part of the signal (e.g., Nostro et al. 1999). Moreover, all the considered source models assume a homogeneous slip on the fault plane, while it is likely that slip values varied on the fault plane, reaching minimum amplitudes at the rupture boundaries. Finally, we must consider that the 1908 tsunami damaged the Messina tide-gauge station, that was restored a few months later; it is not unlikely that in this process a shift of the reference datum has occurred. For these reasons, we expect that modeled coseismic sea level change may be biased by unphysical artifacts that may affect the overall reliability of the inversion. In order to deal with this issue, we carried out two sets of inversions. In the first set, which we consider just for the sake of consistency, we modeled the full sea level signal, including both coseismic and postseismic effects (hereafter CSPS inversion). In the second set, which we expect to give the most reliable results, we modeled only the postseismic response (hereafter PS inversion) by subtracting the respective coseismic offsets from both modeled and observed time-series before the evaluation of eq. 4.

5.1 CSPS inversion

The sampling algorithm results for CSPS inversion in the parameter space $(z, \log(\eta))$, for each of the six source models, are shown in Fig. 5. Red and black circles mark the best fitting and the average models, respectively. The histograms alongside each axis show the marginal distributions of the two variables and give information on the uncertainty associated with the corresponding parameter.

In what follows we will discuss, for each fault model, the results of the parameter space sampling from a visual analysis of Fig. 5. Model S77 is the only case in which we obtain two dis-

tinct minimum regions, both corresponding to the lowest boundary of the viscosity range but with
crustal thicknesses at the lower and upper boundaries of the variability range; the global lowest
misfit values are obtained for low z values. Models B86 and DN91 show a minimum region at the
boundary of the parameter range, both corresponding to the lower limit of crustal thickness. Model
C88 shows a wide minimum region, characterized by a relatively well-defined crustal thickness
($z = 3.64$ km for the best-fitting model), while η is less constrained, ranging from 3.2×10^{17} to
3.2×10^{18} Pa s. Model B89 shows a minimum region characterized by a well-defined viscosity,
with the global minimum at $\eta = 7.9 \times 10^{17}$ Pa s, while the crustal thickness is less constrained
and varies between about 5 and 14 km. Finally, model A02 has a broad minimum region between
viscosities 3.2×10^{17} and 3.2×10^{18} Pa s and crustal thickness between 4 and 14 km. The overall
lowest misfit is obtained with model B89 and corresponds to $z = 5.42$ km and $\eta = 7.9 \times 10^{17}$ Pa
s. In the first three columns of Table 3 we list the best-fitting set of parameters $(z, \log(\eta))$ for each
fault model along with the corresponding misfit value.

In Fig. 6 we compare, for each fault model, the observed postseismic sea level signal ΔS with
its prediction ΔS_{mod} corresponding to the best-fitting parameter values of CSPS inversion. With
the B89 fault model we obtain a sea level prediction in good agreement with observed data, ex-
cept for the first data points that are overestimated by the model. With fault models C88 and A02
the agreement is less satisfactory, even if the long-term sea level rise is correctly recovered. With
model DN91 the temporal dependence of the signal is correctly reproduced but only in the first 4
years of data with a good agreement, whilst the following predicted signal systematically under-
estimates the observations. Using the remaining three fault models, we are not able to reproduce,
even qualitatively, the observed signal, with models S77 and B86 resulting in a sea level fall. In-
cidentally, we observe that these two models are the only ones which suggest a westward dipping
fault.

From Table 3 we can see that for all six source models, the preferred values for crustal thick-
ness are in the lowest region of the variability range, between 2.81 and 5.42 km. Moreover, the
models that can reproduce the features of the observed signal (C88, B89 and A02) indicate a vis-
cosity value in the range between 3.9×10^{17} and 10^{18} Pa s. However, from Fig. 6 we see that

for these models the predicted sea level fails to reproduce the initial part of the signal; this could be explained by an afterslip mechanism acting on short time-scales in addition to viscoelastic relaxation or by the presence of a ductile layer characterized by a transient rheology (Pollitz 2003, 2005; Hetland & Hager 2006; Cannelli et al. 2010). In the latter case, the obtained viscosities would represent a sort of average between the viscosity of transient and steady-state elements.

5.2 PS inversion

Sampling results for PS inversion are shown in Fig. 7, while the best fitting model parameters are reported in Table 3. It is immediately evident that the misfit values obtained from the PS inversion are, for all source models, up to an order of magnitude smaller than corresponding values of CSPS inversion. Best-fitting values of crustal thickness z are generally close to those obtained in CSPS inversion, with the exception of model B89 whose best-fitting z increases from 5.4 to 12.8 km; for the remaining models z is in the range between 2.0 and 5.5 km. The optimal viscosity values are generally different with respect to the CSPS inversion; however, we note that for models C88, B89, DN91 and A02 the range of best-fitting viscosities is quite similar (between 1.4×10^{17} and 3.3×10^{17} Pa s), while for models S77 and B86, best-fitting values of η are similar to those resulting from the CSPS inversion. From a comparison of Figs 5 and 7, we see that the exclusion of coseismic offsets from the modeling has generally reduced the distance between the best-fitting model and the average model, which is an indication of the stability of the inversion process. If we examine from Fig. 7 the distribution of samples in the parameter space, the definition of model parameters is generally similar to the CSPS inversion, even with some exceptions that are worth discussing. Model S77, for which CSPS inversion found two minimum regions, in PS inversion has a single minimum region. In model A02 the minimum region has shifted towards the lower limit of parameter range; the corresponding distribution of viscosities is slightly less defined but those of crustal thickness is improved.

In Fig. 8 we compare the observed and best-fitting modeled signal for all source models. The agreement between the observed postseismic sea level signal ΔS and its prediction ΔS_{mod} is much improved with respect to Fig. 6, proving that the inclusion of coseismic offsets may lead to less

robust results. Models C88, B89, DN91 and A02 reproduce very closely the observed signal. With model S77 the fit in PS inversion is much improved, even if it overestimates the observed signal for the first 10 years of observations, and predicts a stable sea level in the remaining part of the time series. Model B86, as in the CSPS inversion, results in a sea level fall and therefore is not able to reproduce even qualitatively the observed signal.

From Table 3 we see that models C88, DN91 and A02 fit the postseismic signal with very similar values of rheological parameters (z between 3.3 and 5.5 km, η between 1.4×10^{17} and 1.5×10^{17} Pa s). With model B89, we obtain a much larger crustal thickness (12.8km) and a slightly larger viscosity. The remaining two models (S77 and B86) give small values of crustal thickness, while the viscosities are either very small (for model S77) or large (for model B86). If we compare these values with those obtained in CSPS inversion, we see that for models S77 and B86 the best-fitting parameters have not significantly changed from CSPS to PS inversion. For model B89, which also in CSPS inversion gave the largest value of z, crustal thickness increased from 5.4 to 12.8 km, while the viscosity has slightly decreased. For the remaining models (C88, DN91 and A02) the PS inversion gives generally different best-fitting viscosities and slightly larger crustal thicknesses; however, the range of best-fitting parameters for those three models, which was quite scattered in CSPS inversion, is now quite narrow, with z between 3.3 and 5.5 km and $\eta \sim 1.5 \times 10^{17}$ Pa s. The range of crustal thicknesses for these three models is also consistent with average seismic velocity profiles from travel-time tomographic studies in the Calabro-Peloritan region, which suggest a major discontinuity at a depth between 4 and 5 km (e.g., Langer et al. 2007; Barberi et al. 2004).

5.3   Discussion

From the results of the two inversions, we may draw some considerations on the examined source geometries. Models S77 and B86 fail to reproduce the observed sea level signal both in CSPS and PS inversions, even if with model S77 the exclusion of coseismic offsets results in a strong improvement of the fit. It is interesting to remark that these two models are the only ones that assume a westward-dipping fault; the analysis of postseismic sea level seems therefore to exclude this

rupture geometry. The eastward-dipping models (C88, B89, DN91 and A02) are able to reproduce very well the observed signal when only the postseismic component is considered; if the coseismic signal is taken into account, only model B89 gives a satisfactory fit. A likely explanation is that, among all the considered models, only for B89 the Messina tide-gauge is not located within the surface projection of the fault plane and therefore its coseismic prediction could be not affected by spurious boundary effects. However, we note from Table 3 that the estimated crustal thickness for B89 is less stable than other models when the coseismic component is excluded, and results in very large values that are not supported by tomographic evidence. The remaining models (C88, DN91 and A02) are able to reproduce the full signal, even with some limitations, while are in good agreement with data if only the postseismic component is considered. The estimated rheological parameters for those three models in the PS inversions lie in a very narrow range, with z between 2.81 - 5.52 km, and η about 10^{17} Pa s for all three models. It is interesting to note that a common feature of these models is that they suggest a blind shallow rupture, as opposed to model B89 which assumes a deep fault plane.

6 CONCLUSIONS

The aim of this work was to carry out a benchmark on a set of published seismic source models for the 1908 Messina earthquake, in order to check the ability of these models to reproduce the postseismic sea level change observed at the Messina tide-gauge. Since all of the examined source models are based on seismological and leveling data, predictions of postseismic sea level change can represent an independent test for the considered models.

Among the source models proposed in literature in the past decades, we selected a subset of six geometries for which all the needed parameters were defined. These models have been used to fit the postseismic sea level signal at the Messina tide-gauge, through an inversion of a simple rheological profile. We considered both the full sea level signal and its postseismic component alone, in order to take into account effects that may lead to imprecise modeling of near-field coseismic deformations.

From our results, the most robust conclusion is that models S77 and B86, which are the only

ones assuming an westward-dipping fault, fail to predict the observed sea level change, so that this orientation of the seismic source is to be ruled out; this conclusion is in agreement with results obtained from coseismic evidences (e.g., Valensise & Pantosti 1992).

Considering the eastward-dipping source models, we can draw the following considerations: (i) Model B89, which assumes a deep source, fits the observed signal even if the coseismic offset is included. However, the crustal thickness estimate obtained with this model is not stable in the two inversions, and turns out to be quite large (12.8 km) when only the postseismic data is considered, while tomographic studies suggest a major discontinuity between 4 and 5 km. (ii) Models C88, DN91 and A02, which assume a shallow rupture as opposed to model B89, reproduce well the postseismic component of sea level while give a less satisfactory agreement if also the coseismic component is included. With all these models we obtain a crustal thickness within 3.3 and 5.5 km, and a mantle viscosity of about 10^{17} Pa s.

While a final identification of the source model for the Messina earthquake still remains an open issue, we have shown that the analysis of postseismic sea level change can provide an independent benchmark to discriminate among the proposed models, ruling out a class of eastward-dipping fault planes. The assumption of more complex rheological models (for instance by introducing a transient rheology), which was not possible in the present work for computational requirements, may lead to an even more robust identification of a preferred source model.

ACKNOWLEDGMENTS

REFERENCES

Amoruso, A., Crescentini, L., & Scarpa, R., 2002. Source parameters of the 1908 Messina Straits, Italy, earthquake from geodetic and seismic data, *J. Geophys. Res.*, **107**(B4), 2080.

Amoruso, A., Crescentini, L., & Scarpa, R., 2010. Comment on "The 28 December 1908 Messina Straits earthquake (Mw 7.1): A great earthquake throughout a century of seismology", *Seismological Research Letters*, **81**(2), 225–228, 10.1785/gssrl.81.2.225.

Baratta, M., 1910. La catastrofe sismica calabro messinese (28 dicembre 1908), *Relazione alla Società Geografica Italiana*, p. 426.

Barberi, G., Cosentino, M., Gervasi, A., Guerra, I., Neri, G., & Orecchio, B., 2004. Crustal seismic tomography in the Calabrian Arc region, south Italy, *Physics of the Earth and Planetary Interiors*, **147**(4), 297–314.

Bertolaso, G., Boschi, E., Guidoboni, E., & Valensise, G., 2008. Il terremoto e il maremoto del 28 dicembre 1908. analisi sismologica, impatto, prospettive. con dvd-rom, *SGA*, **ISBN:8885213154**, 814.

Billi, A., Funiciello, R., Minelli, L., Faccenna, C., Neri, G., Orecchio, B., & Presti, D., 2008. On the cause of the 1908 Messina tsunami, southern Italy, *Geophys. Res. Lett.*, **35**(6), L06301.

Boschi, E., Pantosti, D., & Valensise, G., 1989. Modello di sorgente per il terremoto di Messina del 1908 ed evoluzione recente dell'area dello Stretto, *Atti VIII Convegno G.N.G.T.S.*, pp. 245–258.

Boschi, E., Guidoboni, E., Ferrari, G., Valensise, G., & Gasperini, P., 1997. Catalogo dei forti terremoti in Italia dal 461 a.C. al 1980, *ING-SGA, Bologna*, **2**, 644.

Bottari, A., Carapezza, E., Carapezza, M., Carveni, P., Cefali, F., Giudice, E. L., & Pandolfo, C., 1986. The 1908 Messina Strait earthquake in the regional geostructural framework, *Journal of Geodynamics*, **5**(3-4), 275–302.

Bottari, A., Capuano, P., De Natale, G., Gasparini, P., Neri, G., Pingue, F., & Scarpa, R., 1989. Source parameters of earthquakes in the Strait of Messina, Italy, during this century, *Tectonophysics*, **166**(1-3), 221–234.

Bottari, A., Carveni, P., Giudice, E. L., Nikonov, A., & Rasà, R., 1992. Anomalous crustal movements prior to great earthquakes as derived from tide-gauge records: the Messina, 1908, *I* = XI, earthquake case history, *Tectonophysics*, **202**(2-4), 269–275.

Cannelli, V., Melini, D., & Piersanti, A., 2010. Post-seismic stress relaxation with a linear transient rheology, *Annals of Geophysics*, **53**(2), 89–99.

Capuano, P., De Natale, G., Gasparini, P., Pingue, F., & Scarpa, R., 1988. A model for the 1908 Messina Straits (Italy) earthquake by inversion of levelling data, *BULLETIN OF THE SEISMOLOGICAL SOCIETY OF AMERICA*, **78**(6), 1930–1947.

Carillo, A., Sannino, G., Artale, V., Ruti, P., Calmanti, S., & Dell'Aquila, A., 2012. Steric sea level rise over the Mediterranean Sea: present climate and scenario simulations, *Climate Dynamics*, **39**(9-10),

2167–2184.

De Natale, G. & Pingue, F., 1991. A variable slip fault model for the 1908 Messina Straits (Italy) earthquake, by inversion of levelling data, *Geophysical Journal International*, **104**(1), 73–84.

Hetland, E. A. & Hager, B. H., 2006. The effects of rheological layering on post-seismic deformation, *Geophysical Journal International*, **166**(1), 277–29.

Langer, H., Raffaele, R., Scaltrito, A., & Scarfi, L., 2007. Estimation of an optimum velocity model in the Calabro-Peloritan mountains-assessment of the variance of model parameters and variability of earthquake locations, *Geophysical Journal International*, **170**(3), 1151–1164.

Loperfido, A., 1909. Livellazione geometrica di precisione eseguita dall'istituto geografico militare sulla costa orientale della Sicilia, da Messina a Castanea, a Gesso ed a Faro Peloro e sulla costa occidentale della Calabria da Gioia Tauro a Melito di Porto Salvo, per incarico del Ministero di agricoltura, industria e commercio, *Relazione della Commissione reale incaricatadi designare le zone più adatte per la ricostruzione degli abitati colpiti dal terremoto del 28 dicembre 1908 o da altri precedenti*, **allegato D**, 131–156.

Melini, D. & Piersanti, A., 2006. Impact of global seismicity on sea level change assessment, *J. Geophys. Res.*, **111**, B03406.

Melini, D., Spada, G., & Piersanti, A., 2010. A sea level equation for seismic perturbations, *Geophysical Journal International*, **180**(1), 88–100.

Mercalli, G., 1909. Contributo allo studio del terremoto calabro-messinese del 28 dicembre 1908, *Atti del Regio Istituto di Incoraggiamento di Napoli*, **s.VI,7**, 249–292.

Mulargia, F. & Boschi, E., 1983. The 1908 Messina earthquake and related seismicity, *Proceedings International School Physics E. Fermi. Earthquakes: observation, theory and interpretation*, pp. 493–518.

Nostro, C., Piersanti, A., Antonioli, A., & Spada, G., 1999. Spherical versus flat models of coseismic and postseismic deformations, *J. Geophys. Res.*, **104**(B6), 13,115ñ13,134.

Olivieri, M., Spada, G., Antonioli, A., & Galassi, G., 2013. Mazara del Vallo tide gauge observations (1906-1916): land subsidence or sea level rise?, *Journal of coastal research*, In Press.

Omori, F., 1913. On the recent sea-level variation at the italian and austrian mareograph stations, and on the cause of Messina-Reggio earthquake of 1908., *Bull. Imp. Earthquake Invest. Comm.*, **5**, 87–100.

Piatanesi, A., Tinti, S., & Bortolucci, E., 1999. Finite-element simulations of the 28 December 1908 Messina Straits (southern Italy) tsunami, *Physics and Chemistry of the Earth, Part A: Solid Earth and Geodesy*, **24**(2), 145–150.

Pinardi, N., Korres, G., Lascaratos, A., Roussenov, V., & Stanev, E., 1997. Numerical simulation of the interannual variability of the Mediterranean Sea upper ocean circulation, *Geophys. Res. Lett.*, **24**(4), 425–428.

Pino, N., Giardini, D., & Boschi, E., 2000. The December 28, 1908, Messina Straits, southern Italy,

earthquake: Waveform modeling of regional seismograms, *J. Geophys. Res.*, **105**(B11), 25,473–25,492.

Pino, N., Piatanesi, A., Valensise, G., & Boschi, E., 2009. The 28 December 1908 Messina Straits earthquake (Mw 7.1): A great earthquake throughout a century of seismology, *Seismological Research Letters*, **80**(2), 243.

Pino, N., Piatanesi, A., Valensise, G., & Boschi, E., 2010. Reply to "Comment on 'The 28 December 1908 Messina Straits earthquake (Mw 7.1): A great earthquake throughout a century of seismology'", *Seismological Research Letters*, **81**(2), 229–231, 10.1785/gssrl.81.2.229.

Platania, G., 1909. Il maremoto dello Stretto di Messina del 28 dicembre 1908, *Bollettino della Società Sismologica Italiana*, **13**, 369–458.

Pollitz, F., 2003. Transient rheology of the uppermost mantle beneath the Mojave Desert, California, *Earth and Planetary Science Letters*, **215**(1-2), 89ñ104.

Pollitz, F. F., 2005. Transient rheology of the upper mantle beneath central Alaska inferred from the crustal velocity field following the 2002 Denali earthquake, *J. Geophys. Res.*, **110**(B08407).

Sambridge, M., 1999a. Geophysical inversion with a neighbourhood algorithm - I. Searching a parameter space, *Geophysical Journal International*, **138**(2), 479–494.

Sambridge, M., 1999b. Geophysical inversion with a neighbourhood algorithm - II. Appraising the ensemble, *Geophysical Journal International*, **138**(3), 727–746.

Schick, R., 1977. Eine seismotektonische Bearbeitung des Erdbebens von Messina im Jahre 1908, *Geol. Jahrb. R. E.*, **H**(11), 3–74.

Spada, G. & Stocchi, P., 2006. The sea level equation, theory and numerical examples, *Aracne Roma*, **ISBN: 8854803847**, pages 96.

Tinti, S., Armigliato, A., Bortolucci, E., & Piatanesi, A., 1999. Identification of the source fault of the 1908 Messina earthquake through tsunami modelling. Is it a possible task?, *Physics and Chemistry of the Earth, Part B: Hydrology, Oceans and Atmosphere*, **24**(5), 417–421.

Valensise, G., 1988. Low angle normal faulting during the 1908, Messina earthquake revealed by geodetic data analysis, *Eos Trans. AGU*, **69**(44), 1433.

Valensise, G. & Pantosti, D., 1992. A 125 kyr-long geological record of seismic source repeatability: the Messina Straits (southern Italy) and the 1908 earthquake (Ms= 7.5), *Terra Nova*, **4**(4), 472–483.

Wang, R., Lorenzo-Martín, F., & Roth, F., 2006. PSGRN/PSCMP a new code for calculating co- and post-seismic deformation, geoid and gravity changes based on the viscoelastic-gravitational dislocation theory, *Computers & Geosciences*, **32**(4), 527–541.

Woodworth, P. L. & Player, R., 2003. The Permanent Service for Mean Sea Level: An update to the 21st century, *Journal of Coastal Research*, **19**(2), 287–295.

Table 1. Source parameters for fault models considered in this study. Seismic moment values (M_0) for all models and fault plane orientations for models S77, C88, B89 and A02 are from Table 2 of Pino et al. (2009); all the remaining parameters are derived from corresponding references.

		M_0	Strike	Dip	Rake	Fault size	Top depth
		$(10^{19} Nm)$		(deg)		($l \times w$, km^2)	(km)
S77	Schick (1977)	4.4	195	70	-90	30×15	0
B86	Bottari et al. (1986)	5.1	222	59	-90	50×20	16
C88	Capuano et al. (1988)	4.9	355.8	38.6	-132.5	56.7×18.5	1.1
B89	Boschi et al. (1989)	3.7	11.5	29	- 90	45×18	4
DN91	De Natale and Pingue (1991)	3.5	355.8	38.6	-132.5	70×30	1.1
A02	Amoruso et al. (2002)	2.4	-5.5	42.4	-118.3	29.8×19.8	1.5

Table 2. Rheological structure employed in this study. Upper crust thickness z is varied between 2 and 20 km. Lower crust viscosity η is sampled logarithmically, with $\log(\eta/1\ Pa\ s)$ varying between 16 and 19.

Layer	Depth (km)	Vp (km/s)	Vs (km/s)	Density $(10^3 kg/m^3)$	Viscosity (Pa s)
1. Crust	$0-z$	7.08	3.94	3.1	0
2. Upper mantle	$z-220$	8.05	4.45	3.4	η
3. Lower mantle	$220-\infty$	9.36	5.06	3.7	10^{20}

Table 3. Summary of the best-fitting rheological parameters for the considered source models. Chi-square values are evaluated according to eq. 4, subtracting the coseismic terms for CSPS inversions.

Model	CSPS inversion			PS inversion		
	χ^2	z	$\log(\eta/1\ Pa\ s)$	χ^2	z	$\log(\eta/1\ Pa\ s)$
	$(\times 10^4)$	(km)		$(\times 10^4)$	(km)	
S77	286	3.2	16.0	46.6	3.4	16.5
B86	1923	3.2	19.0	1363.7	2.0	19.0
C88	18	3.6	18.0	7.7	5.5	17.1
B89	10	5.4	17.9	7.3	12.8	17.5
DN91	72	2.8	16.2	7.3	3.3	17.2
A02	22	3.7	17.6	8.3	5.3	17.2
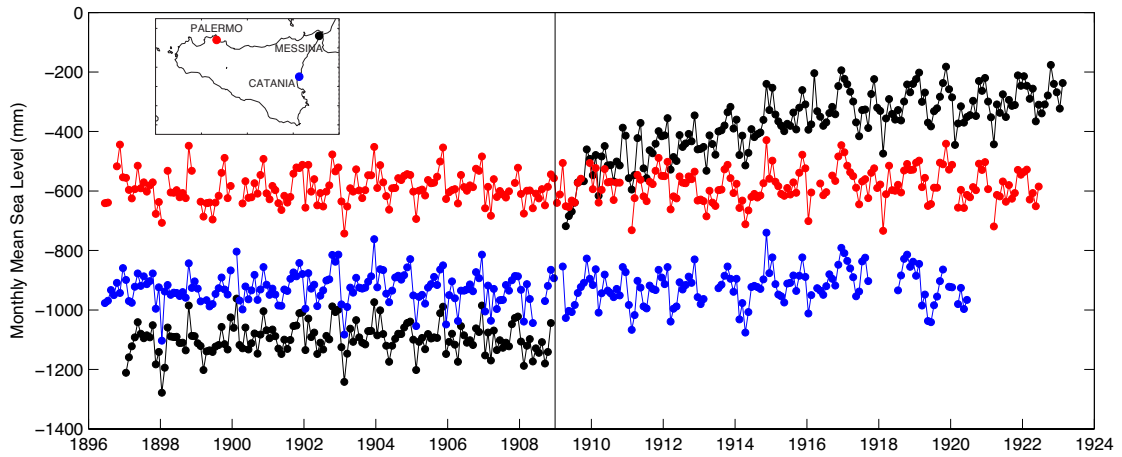
Figure 1. Monthly mean values of sea level from tide gauge stations of Messina (black circles), Palermo (red circles) and Catania (blue circles). The vertical black line marks the occurrence of the Messina earthquake (December 28th, 1908). The locations of the three tide gauge stations are shown in the inset.
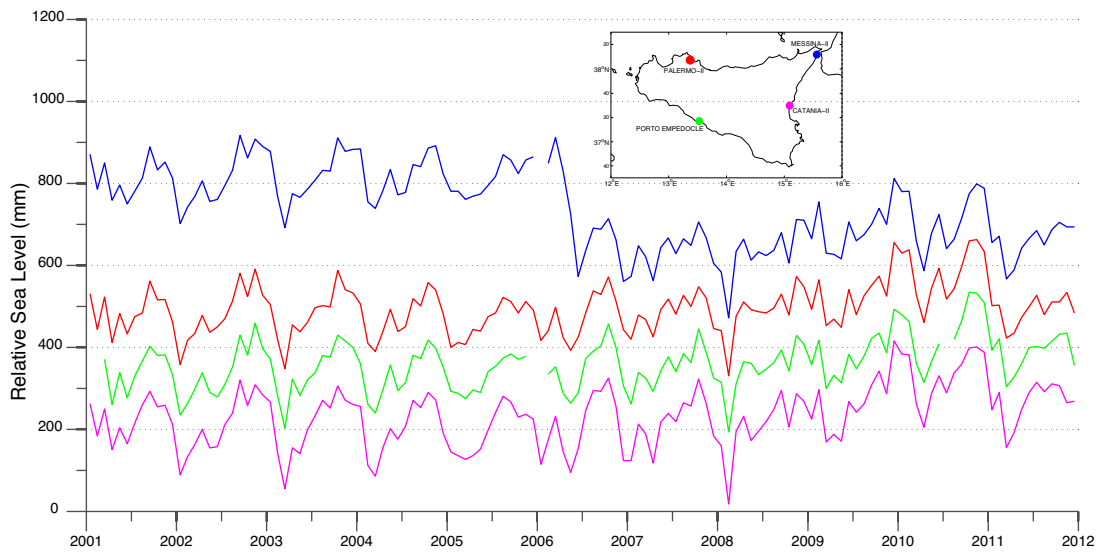
Figure 2. Time series (PSMSL data) for the period 2001-2012 for tide gauge stations in Sicily (Palermo-II, Porto Empedocle, Catania-II and Messina-II). Corresponding tide gauge positions are shown in the inset.
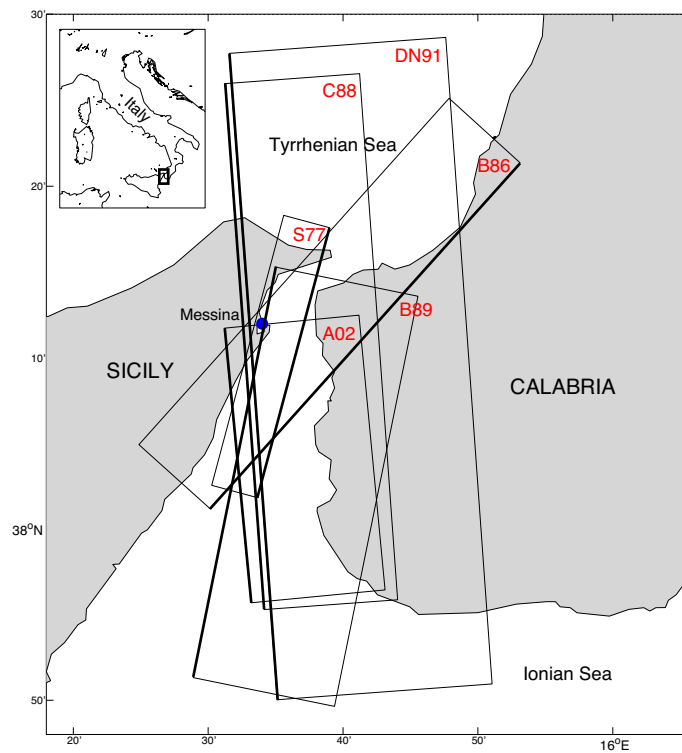
Figure 3. Relative location of the source models considered in this study for the 1908 Messina earthquake. The shallow edge of each source model is marked by a thick line. The blue circle shows the location of the city of Messina.
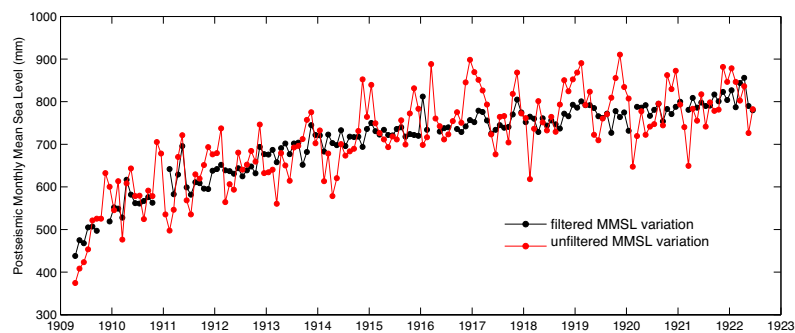
Figure 4. Monthly Mean Sea Level (MMSL) variation at Messina tide gauge station before (red circles) and after (black circles) tidal filtering, according to eq. 3.
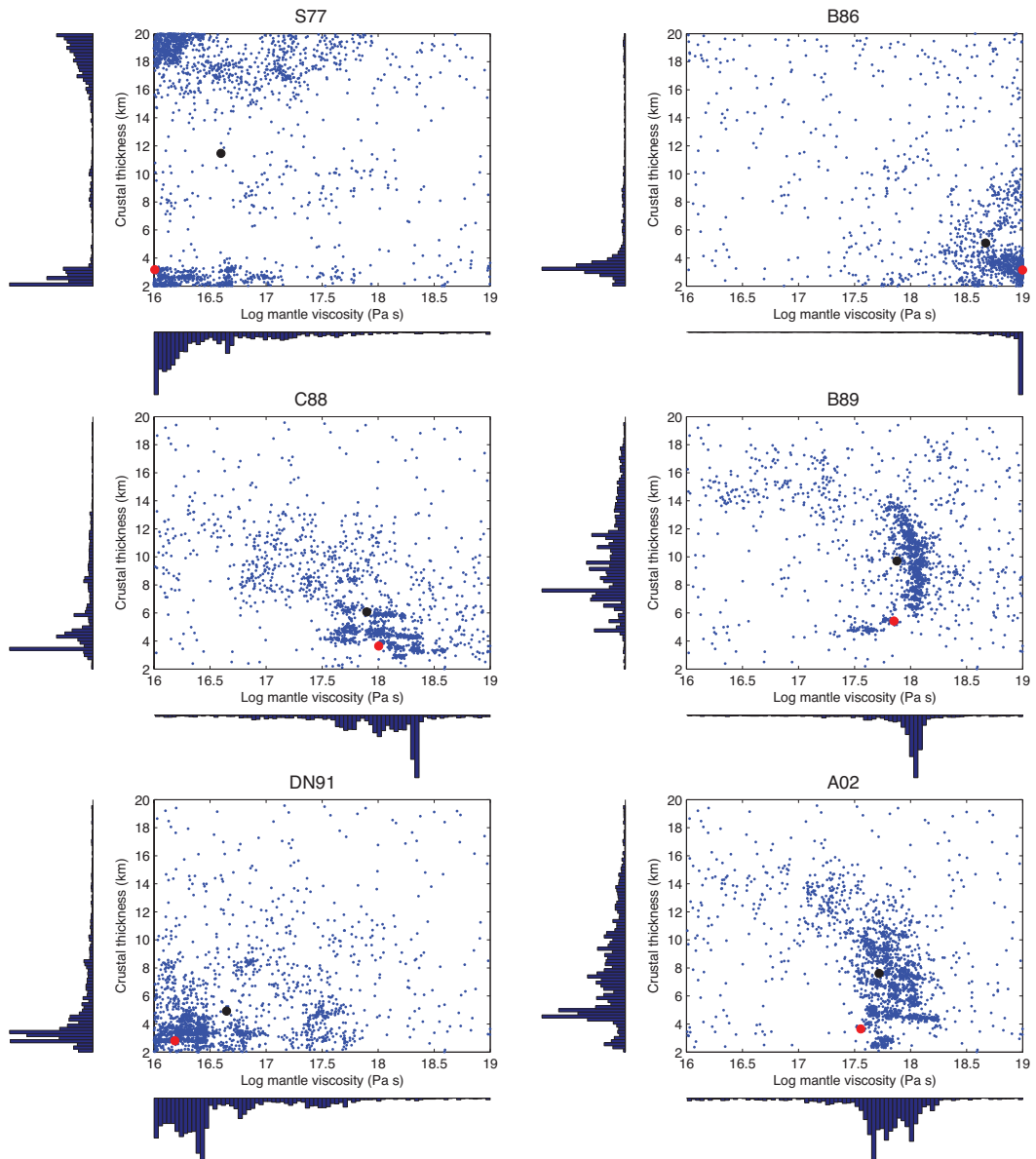
Figure 5. Distribution in the parameter space $(\log(\eta), z)$ of the 2200 models produced for each source model by CSPS inversion. In each panel red and black circles mark, respectively, the best and the average models. The histograms alongside each axis show the distributions of the sampled parameters.
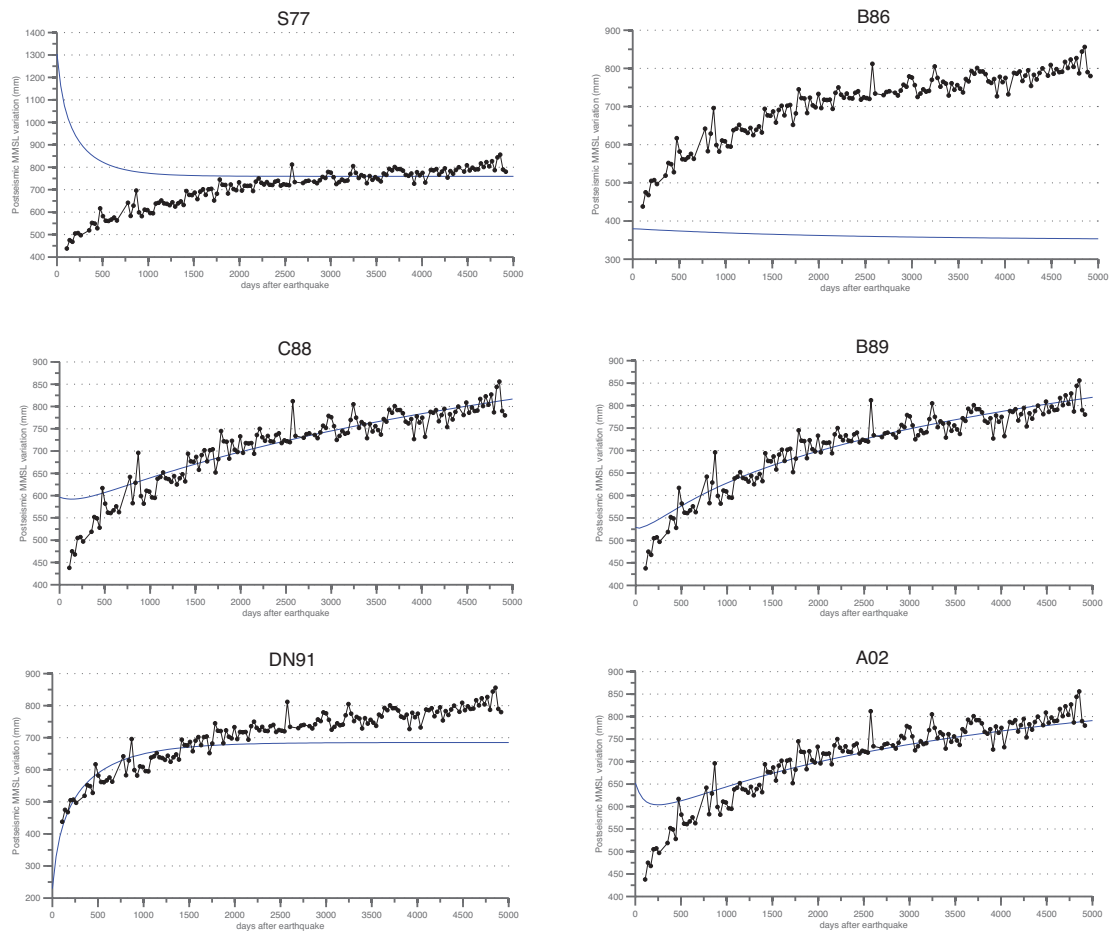
Figure 6. Comparison between observed (black) and predicted (blue) sea level variations for each of the considered source models. Predicted signal is computed with the best-fitting model parameters obtained in CSPS inversion.
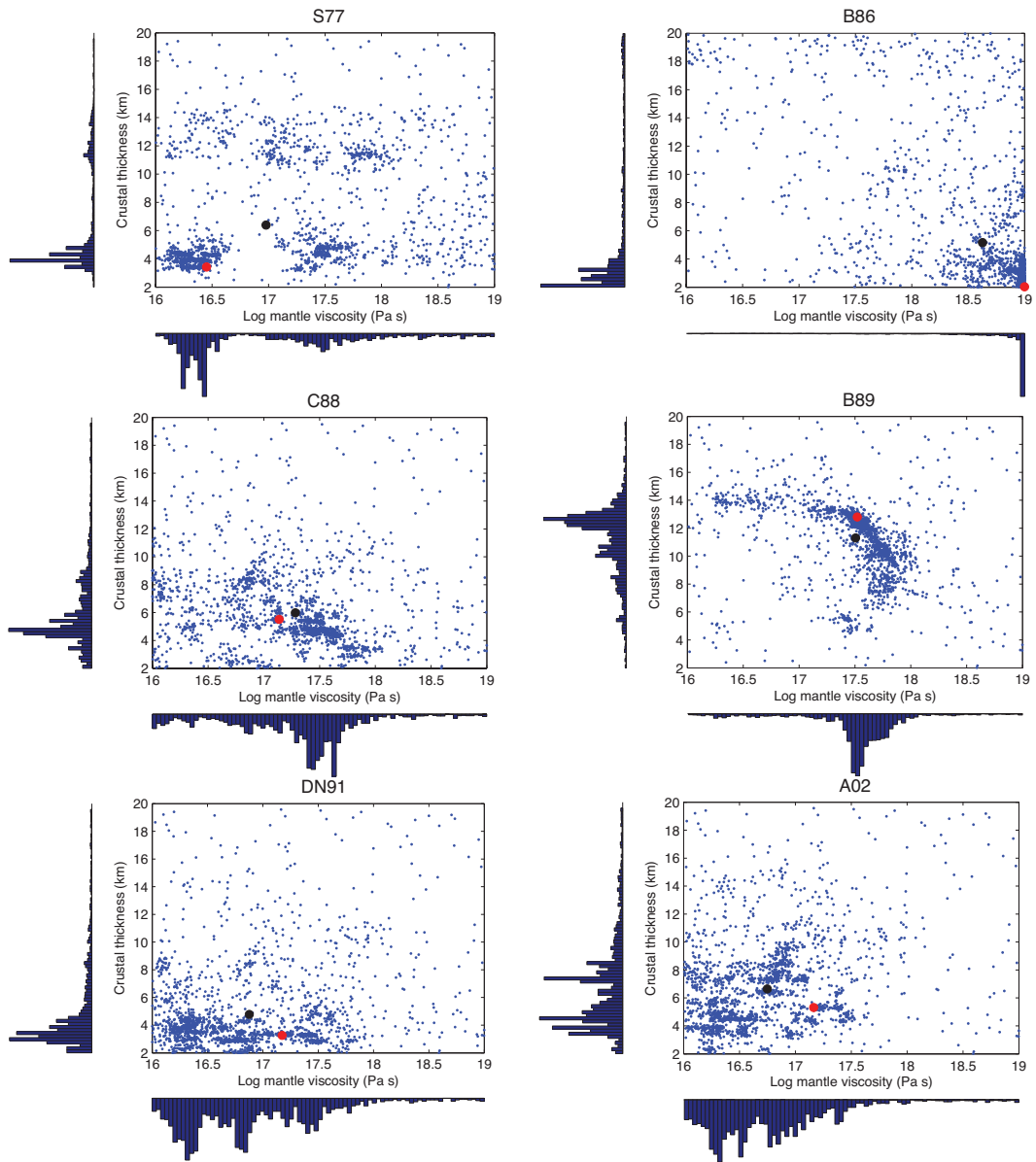
Figure 7. Distribution in the parameter space of the model samples for PS inversion. See also caption of Fig. 5.
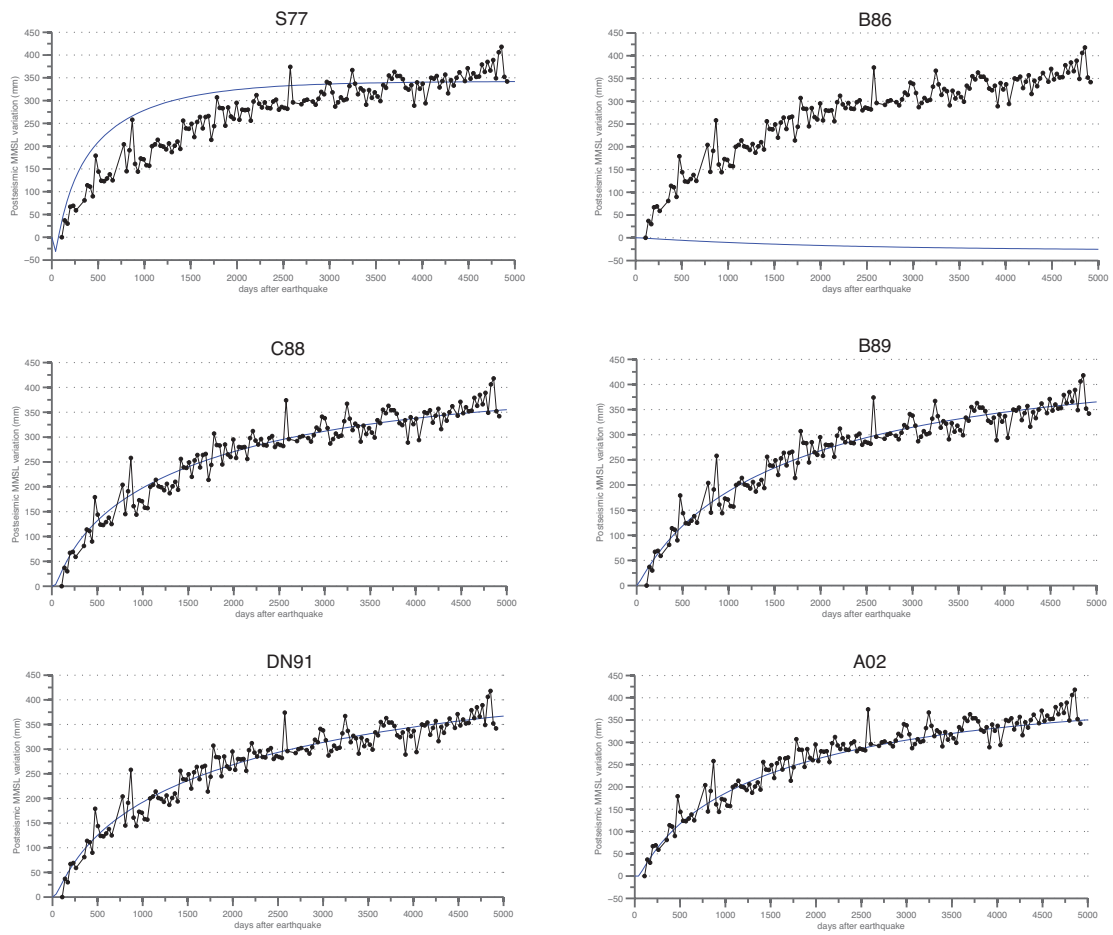
Figure 8. Comparison between observed and predicted sea level for PS inversion. See also caption of Fig. 6.